


Rapid and label-free urine test based on surface-enhanced Raman spectroscopy for the non-invasive detection of colorectal cancer at different stages

JINYONG LIN,^{1,2,4,5} ZONGWEI HUANG,^{1,4} XUELIANG LIN,² QIONG WU,² KERUN QUAN,³ YANMING CHENG,¹ MINGZHI ZHENG,¹ JIAYING XU,¹ YITAO DAI,¹ HEJIN QIU,¹ DUO LIN,^{2,6}  AND SHANGYUAN FENG^{2,7}

¹Radiation Oncology Department, Fujian Cancer Hospital & Fujian Medical University Cancer Hospital, Fuzhou, 350014, China

²Key Laboratory of OptoElectronic Science and Technology for Medicine, Ministry of Education, Fujian Provincial Key Laboratory for Photonics Technology, Digital Fujian Internet-of-Things Laboratory of Environment Monitoring, Fujian Normal University, Fuzhou, 350007, China

³School of Nuclear Science and Technology, University of South China, Hengyang 421001, China

⁴These authors contributed equally to this work

⁵linjyphysics@sina.cn

⁶duo@fjnu.edu.cn

⁷syfeng@fjnu.edu.cn

Abstract: The concept of being able to urinate in a cup and screen for colorectal cancer (CRC) is fascinating to the public at large. Here, a simple and label-free urine test based on surface-enhanced Raman spectroscopy (SERS) was employed for CRC detection. Significant spectral differences among normal, stages I-II, and stages III-IV CRC urines were observed. Using discriminant function analysis, the diagnostic sensitivities of 95.8%, 80.9%, and 84.3% for classification of normal, stages I-II, and stages III-IV CRC were achieved in training model, indicating the great promise of urine SERS as a rapid, convenient and noninvasive method for CRC staging detection.

© 2020 Optical Society of America under the terms of the [OSA Open Access Publishing Agreement](#)

1. Introduction

Worldwide, colorectal cancer (CRC) has become the third cause of cancer incidence and the second cause of cancer mortality, with about 1.8 million new CRC cases and 881,000 deaths occurred in 2018 [1]. The cancer staging (I, II, III, and IV) closely correlates with prognosis and is the most significant predictor of the survival in patients with CRC. The 5-year relative survival rate for CRC patients with stage I or II disease are 91% and 82%, respectively. However, 5-year survival rate declines to 12% for stage IV disease [2]. So early diagnosis plays a significant role in improving therapeutic efficacy and survival rate for CRC patients. Currently, the routine approaches for CRC detection are the fecal occult blood test (FOBT) and the colonoscopy. However, these methods have certain inadequacies [3]. For example, the sensitivity and specificity of FOBT are lower, particularly for early stage patients who usually do not bleed. The procedures of colonoscopy are complex, time-consuming, expensive, invasive and uncomfortable for patients, resulting in poor compliance rates. Accordingly, there is a urgent need to develop a rapid, convenient, noninvasive and accurate test to promote the CRC detection.

Surface-enhanced Raman spectroscopy (SERS), which is based on inelastic scattering light, is a rapid, noninvasive and ultra-sensitive bioanalytical technique [4,5]. When the biomolecules are adsorbed onto the gold or silver nanoparticles surface, the Raman signals of the biomolecules

will be dramatically amplified to 11-15 orders of magnitude, yielding rich chemical fingerprint information of biomolecules, such as DNA, RNA, protein and lipid [6–9]. Recently, SERS has attracted increasing interest in biomedical research and is emerging as a potentially useful clinical adjunct in cancer diagnosis, capable of identifying the subtle changes associated with cancer progression in biological samples, such as tissue, cell, blood, urine, and saliva [5,10–19]. Specially, for CRC detection, blood SERS was firstly applied to successfully differentiate the blood from CRC patients and healthy volunteers by our group in 2011 [20]. Subsequently, blood RNA SERS and blood protein SERS were also employed to detect CRC, and satisfying detection results were obtained [21,22]. However, it should be pointed out that human urine is a more ideal medium for cancer detection due to its noninvasive, abundant and facile collection procedure than blood. Importantly, urine is the product of human metabolism from the blood, which makes it contains many biological molecules (e.g. DNA, RNA, protein [23–25]) that can timely reflect human's health condition. Application of urine SERS for cancer detection has been reported on prostate cancer [18], breast cancer [26], and esophagus cancer [17] by Mistro's group, Moisoiu's group, and our group. These exploratory efforts demonstrated urine SERS method was extremely promising for cancer detection. However, these reported researches on urine SERS only focused on preliminary recognition of cancer group from normal group. There are little studies exploring further on the feasibility of applying urine SERS for cancer detection at different stages which is the most important prognostic factor and has high directive value in making therapy plan.

Hence, this study aimed to evaluate the feasibility of applying gold nanoparticles (Au-NPs) based SERS techniques for label-free analysis of urine samples belonging to normal, early (stages I-II), and advanced (stages III-IV) colorectal subjects for CRC staging detection. The principal component analysis and discriminant function analysis (PCA-DFA) multivariate methods were employed to analyze and discriminate the urine SERS spectra acquired from the three groups. To the best of our knowledge, this is the first report on urine SERS for CRC detection, especially for cancer staging detection which is important for clinician to assess the patient's status and make optimal therapy decision. This primary study may develop a rapid, convenient and noninvasive method for CRC detection at different stages.

2. Materials and methods

2.1. Preparation and characterization of Au-NPs

Stable Au colloid was synthesized following the method reported by Grabar's group [27]. Briefly, 100 mL HAuCl₄ solution (1 mM) was brought to a rolling boil with continuous stirring. Then, 10 mL sodium citrate solution (38.8 mM) was brought to the above solution quickly, and the mixture was kept boiling and stirring for 15 mins until a homogenous sol with a burgundy color was obtained. The Au colloid was characterized by the transmission electron microscopy and the ultraviolet-visible absorption spectrum. Before use as SERS substrate, gold colloid was centrifuged at 12000 rpm for 10 mins. After centrifugation, the supernatant were removed and the volume ratio of supernatant to sediment is 49:1. The final concentration of gold colloid is about 8.87×10^{11} /mL.

2.2. Collection and preparation of urine samples

In this study, a total of 116 human urine samples were collected from two subject groups: one consisted of healthy volunteers (n=53), the other with histopathological diagnosis of colorectal cancer (n=63). According to the eighth edition of the International Union Against Cancer/American Joint Committee on Cancer staging system [28], 26 cancers were I-II stages and 37 cancers were III-IV stages. All cancer subjects were first diagnosed with CRC (without undergo any drug treatments). All subject groups took part in the examination of colonoscopy. The detailed information on subjects can be found in Table 1. All urine samples were from the

Fujian Cancer Hospital (Fuzhou, China), and the research was approved by the ethical committee in the hospital (No. 2017-070-01). All urine samples were collected based on the same procedure. Firstly, after 12 hours of overnight fasting, 2 mL urine was obtained from study subjects between 6:30 A.M. and 8:30 A.M. And then, each urine sample was immediately centrifuged at 10000 rpm for 10 mins to remove the impurities (including cell debris) after collection. Before SERS measurement, 5 μ L urine and 5 μ L Au colloid were mixed. Then, a drop of this mixture was pipetted onto an aluminum slide and air-dried for SERS analysis. Three measurements from the different edge region of the dried sample were taken to obtain each data point. Figure 1 illustrated the preparation of urine/Au-NPs analyte for SERS measurement and statistic analysis.

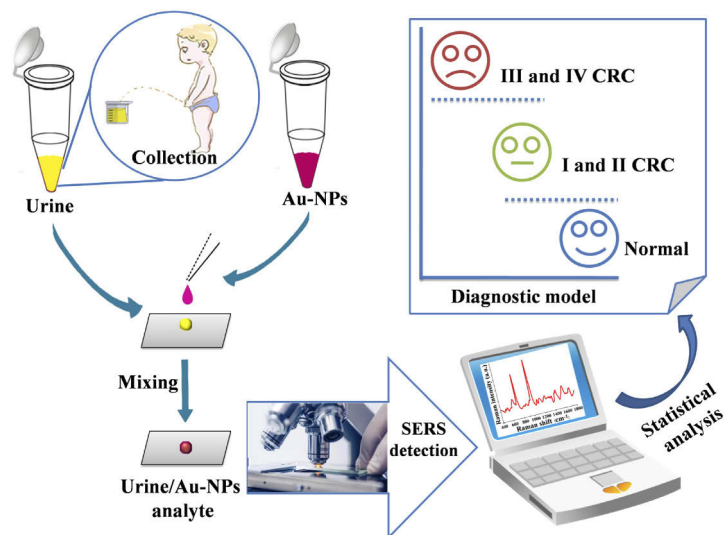


Fig. 1. The schematic representation of the measurement and analysis of Au-NPs based SERS spectra for CRC detection at different cancer stages

Table 1. Clinical information on CRC and healthy subjects^a

	CRC patients (n=63)	Healthy subjects (n=53)
Age		
Mean	51 \pm 7	49 \pm 9
Gender		
Male	34	27
Female	29	26
TNM stage		
I and II	26	N/A
III and IV	37	N/A

^aNote: N/A is the abbreviation for “not applicable”

2.3. SERS spectral measurement

A confocal Raman micro-spectrometer (Renishaw, Great Britain) equipped with a Peltier cooled charge-coupled device camera (spectral resolution of 2 cm^{-1}) was used for SERS measurement. Urine SERS spectra were generated by a 785 nm diode laser (about 1.0 mW power) through a Leica 20 \times objective and were recorded from 400 to 1800 cm^{-1} with 10 s exposure time. 785 nm

excitation can efficiently reduce the biological autofluorescence and the scattering background from surrounding medium or solvent [29], which has been widely applied in SERS analysis for biological samples in biomedical research [5,16,29]. The Renishaw software package WIRE 3.4 was employed for SERS acquisition and analysis. Prior to SERS measurement, the instrument response and wavelength position were calibrated by the 520 cm^{-1} band of the silicon wafer.

2.4. Data processing and analysis

For a better comparison of spectral shapes and relative intensities of the measured SERS bands among stages III-IV CRC, stages I-II CRC, and healthy urine samples, raw spectral data were processed using a fifth-order multi-polynomial fitting algorithm [30] to subtract the fluorescence background. After that, all above spectra were normalized to the integrated area under the curve range within 400 to 1800 cm^{-1} . After normalizing the spectral area to a value of 1, the spectral intensity value represents the percentage signals of Raman bands. By this way, the absolute intensity variations from laser fluctuations and sample concentration inhomogeneity can be cancelled, which helps comparing the variation in relative compositions and structures between different urine samples [31]. Ultimately, the processed spectral data were put into the SPSS statistic software (SPSS Inc., Chicago) for PCA-DFA.

3. Results and discussion

3.1. SERS spectral analysis

SERS is an ultra-sensitive bioanalysis tool resulting in strongly increased Raman signals from biomolecules attached to nanometer sized metallic surface. In this study, the Au-NPs with a mean diameter of $43 \pm 6\text{ nm}$ [in Fig. 2(A)] and a maximum absorption peak at 527 nm [in Fig. 2(B)] were used as SERS substrate. To study the Au-NPs enhancement effect on the urine, drops of Au-NPs, the urine without Au-NPs, and the 1:1 urine-Au-NPs mixture were pipetted onto an aluminum slide for SERS analysis under the same measuring condition, respectively. In Fig. 3(A), line I, II, and III represented the SERS spectrum of urine, the regular Raman spectrum of urine without Au-NPs, and the background Raman signal of the Au-NPs, respectively. By comparing between the urine SERS spectrum and regular Raman spectrum, it showed that urine SERS spectrum owned more intense and sharp peaks than urine regular Raman spectrum, revealing that many molecular vibration bands have been enhanced remarkably by SERS and there was an interaction between urine molecules and Au-NPs. One possible explanation for this enhancement is the significant magnification of the local electromagnetic field from the interspaces between concentrated Au-NPs (i.e. the so-called “hot spot”) [32]. Meanwhile, there were hardly any background Raman signals (in 400 - 1800 cm^{-1} range) from the Au-NPs substrate [line III in Fig. 3(A)]. Based on excellent enhancement performance, Au-NPs based SERS technique has been widely used for the cancer detection in current biomedical research field [20,33–35].

Figure 3(B) showed a comparison of the normalized average SERS spectra from 37 stages III-IV CRC, 26 stages I-II CRC, and 53 healthy urine samples using Au-NPs as SERS substrate, respectively. The corresponding standard deviations (the shaded areas) displayed that each group had a relatively good spectral reproducibility within intra-group, assuring a better comparison of the spectral characteristics among different groups. The average urine SERS spectra of the three groups exhibited primary characteristic peaks at 495 , 527 , 640 , 683 , 725 , 828 , 889 , 1002 , 1090 , 1130 , 1241 , 1358 , 1426 , 1455 , 1596 , and 1706 cm^{-1} with the strongest SERS peaks at 725 and 1002 cm^{-1} . The spectral assignments were listed in Table 2, according to the previous researches [36–40]. The spectra contained most information related to the biomolecules such as amino acids, urea, uric acid, creatinine, DNA/RNA bases and so on which are the major contents of human urine. To highlight the spectral differences among the three groups, the difference spectra were shown in Fig. 3(C). It can be found that CRC urine samples showed higher intensities at 495 , 640 ,

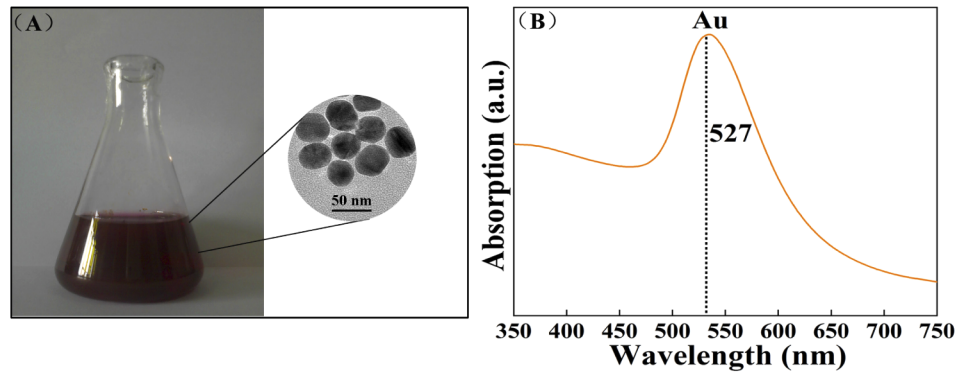


Fig. 2. (A) The photograph of the Au colloid with a burgundy color and the inserted picture is the transmission electron microscopy micrograph. (B) The ultraviolet-visible absorption spectrum of the Au colloid. The maximum absorption peak is localized at 527 nm.

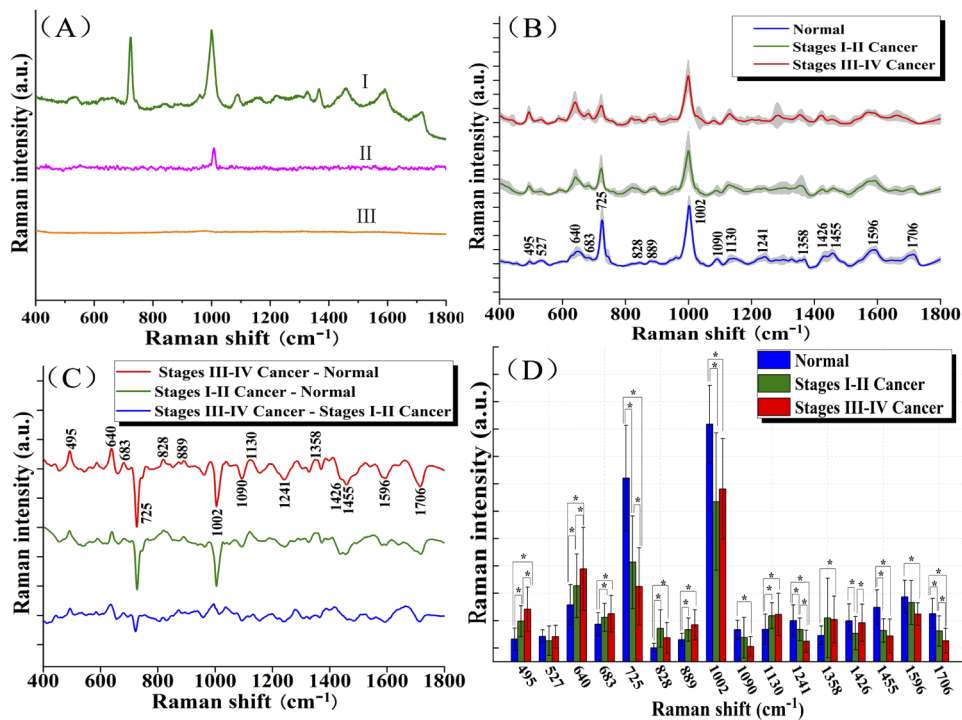


Fig. 3. (A) Spectra taken from the urine and Au-NPs mixture (I), the urine sample without Au-NPs (II), and Au-NPs enhanced substrate (III) under the same measuring condition. (B) Comparison of the normalized average SERS spectra from 37 stages III-IV CRC, 26 stages I-II CRC, and 53 healthy urine samples, respectively. In addition, the standard deviations are represented by the shaded areas. (C) The difference spectra calculated from the mean SERS spectra among the three groups. (D) The corresponding histograms of the average intensities and standard deviations of SERS peaks among the three groups. * $p < 0.05$

683, 828, 889, 1130, and 1358 cm^{-1} , while lower at 725, 1002, 1090, 1241, 1426, 1455, 1596, and 1706 cm^{-1} as compared with healthy samples. In addition, the intensities of SERS peaks at 495, 640, 683, 725, 889, 1090, 1130, 1241, 1455, 1596, and 1706 cm^{-1} showed linear changes as cancer staging development (from stages I-II to stages III-IV). Figure 3(D) was the histogram of the average intensity values of urine SERS peaks with associated standard deviations. The significantly different peaks among the three groups were identified by one-way analysis of variance with the definition of p-value (i.e. probability) <0.05 . These variations showed the componential changes of urinary biomolecules with colorectal neoplasia progress. For instance, the higher spectral intensity of uric acid (at 640 and 1130 cm^{-1}) for the CRC patients indicated there was an increase of uric acid content relative to the total SERS-active components in CRC urine, which was in accordance with previous SERS study on urine of prostate cancer [18]. In addition, previous studies also have reported that the upraised uric acid level was a risk indicator for the precursor of CRC [41]. The SERS peak at 1002 cm^{-1} due to the urea [39] showed lower signal in CRC group, suggesting that the relative amounts of urea were less in colorectal urine, which is consistent with previous urinary metabolomic study on CRC urine by mass spectrometry [42]. Similar change in this peak was also found in our previous urine SERS analysis of other cancer [17]. The band at 828 cm^{-1} , which can be assigned to glutathione, exhibited higher signal in colorectal patients. Barranco et al. [43] and Qiu et al. [44] also observed a significant increase of glutathione in CRC tissues and urine, respectively, when compared to the corresponding normal samples. The possible mechanism for the higher level of glutathione (an antioxidant) may be indicative of increased oxidative stress in tumor microenvironment. Moreover, the SERS bands of tryptophan (495, 683, and 1358 cm^{-1}), histidine (1090 cm^{-1}), tyrosine (1241 cm^{-1}), guanine (495 and 1358 cm^{-1}), uracil (1455 cm^{-1}) and DNA/RNA bases (725 and 1241 cm^{-1}), which were significantly up-regulated or down-regulated in cancer group, suggesting that there were dysregulated metabolism of specific amino acids and nucleic acid bases in CRC urine. These changes were also discovered by previous researches on urinary metabolomic and modified nucleoside of CRC patients [44,45]. In particular, for tryptophan metabolism which is a key regulator of inflammation and immunity, the up-regulated tryptophan metabolism may be a body's defense reaction to improve the intestinal epithelial barrier function and reduce the inflammation response which were usually occurred with the development of CRC [46]. These above reproducible variations in urine SERS spectra among different cancer stages of CRC patients and healthy subjects suggested the potential of Au-NPs based SERS method for rapid and convenient detection of colorectal cancer.

3.2. Multivariate statistical analysis

In order to automatically extract and incorporate all diagnostically significant signatures from the whole SERS spectra for promoting the efficient detection of colorectal cancer, PCA-DFA statistical algorithms were executed on the urine SERS spectra by SPSS 15.0 software package (SPSS Inc. Chicago). Currently, PCA-DFA based statistical method has been widely applied for cluster analysis of spectral data [47]. As a dimensional-reduction tool, PCA extracted the meaningful information out of a complex set of spectral data variables, conveying it in a minimal set of orthogonal variables called principal components (PCs) [48]. Meanwhile, As a classification method, DFA could maximize the ratio of between-class variance to within-class variance in a dataset to give the best discrimination between the classes [10,49]. In this study, 116 SERS spectral data (37 stages III-IV CRC, 26 stages I-II CRC, and 53 healthy) were divided into a training set (32 stages III-IV CRC, 21 stages I-II CRC, and 48 healthy) and a validation set (5 stages III-IV CRC, 5 stages I-II CRC, and 5 healthy) for statistical analysis. The training dataset was used to establish a discrimination model for CRC detection and the validation dataset was used to evaluate the performance of the discrimination model. Firstly, PCA was used to the multidimensional spectral data (400-1800 cm^{-1}) to generate 47 PCs which can explain

Table 2. The tentative assignments for urine SERS spectra

Raman shift (cm ⁻¹)	Tentative assignment ^a
495	Guanine, Tryptophan
527	Nucleic acids, Glutamate
640	Uric acid
683	Tryptophan
725	DNA/RNA bases, Hypoxanthine
828	Glutathione
889	D-Galactosamine, Glycine
1002	Urea
1090	Phosphate, Histidine
1130	Uric acid
1241	Tyrosine, RNA
1358	Guanine, Tryptophan
1426	Creatinine, Valine
1455	Uracil
1596	Alanine, Serine
1706	Creatinine

^a Assignments taken from References [36–40].

98.7% of total variance. Next, one-way analysis of variance was conducted on these 47 PCs to determine the most diagnostically significant PCs for distinguishing among the stages III-IV CRC, stages I-II CRC, and healthy urine samples using the definition of $p < 0.05$ [50]. As a result, PC2, PC3, PC8, PC18, PC24, PC25, PC29, and PC43 were calculated to be the most diagnostically significant PCs, which accounted for 30.63% of the total variance. Figure 4(A) was the plot of these most diagnostically significant PCs. The plot enabled one to know which spectral variables are dominating or influencing the PCA-DFA model. It was clear that these diagnostically significant PCs shared most peaks in the difference spectra in Fig. 3(C), including 495, 640, 683, 725, 828, 889, 1002, 1090, 1130, 1241, 1358, 1426, 1455, 1596, and 1706 cm⁻¹, which were diagnostically relevant spectral peaks. Then, these most diagnostically significant PCs were loaded into DFA model for discriminating among the three groups. As a result, two canonical discriminant functions were calculated [shown in equation (S1)]. In the training stage, the 32 stages III-IV CRC, 21 stages I-II CRC, and 48 healthy data were backtracked separately to the DFA model to self-assess the performance of the model. The sensitivities of 95.8%, 80.9%, 84.3%; and the specificities of 94.3%, 95.0%, 94.2%, respectively, were achieved for classification of normal, stages I-II CRC, and stages III-IV CRC subjects in training model, showing a relatively satisfactory result. These statistical results were summarized in Table 3. Then, in the validation stage, double-blind tests were performed on the additional 5 stages III-IV CRC, 5 stages I-II CRC, and 5 healthy subjects. After adding the additional SERS data into the above discrimination model, classification results against clinical information were reached for 5 out of 5 healthy, 4 out of 5 stages I-II CRC and 4 out of 5 stages III-IV CRC. The diagnostic sensitivities were 100%, 80%, 80%; and the specificities were 90%, 90%, 100%, respectively. The specific results were shown in Table S1. Figures 4(B) and 4(C) were the scatter plot of the discrimination scores and the ternary plot of the posterior probabilities for training dataset and validation dataset, demonstrating the good clustering (with overlap slightly) of the three distinctive groups achieved by the PCA-DFA diagnostic algorithms. Finally, the

receiver operating characteristic (ROC) curves [shown in Fig. 4(D)], which were the plots of tests' sensitivities versus their false-positive rates for all possible threshold levels [51], were generated to further assess the performance of PCA-DFA model for CRC detection. The area under the ROC is positively related with the detection accuracy. Here, areas under the ROC curves were 0.991, 0.959 and 0.961, respectively, all close to 1 (the maximum value), for the three groups' classification, demonstrating relatively ideal discrimination model based on PCA-DFA. This work indicated the promising potential of urine SERS spectra combined with PCA-DFA as label-free analytical method for componential analysis of human urine for promoting the rapid, convenient and noninvasive detection of colorectal cancer at different stages.

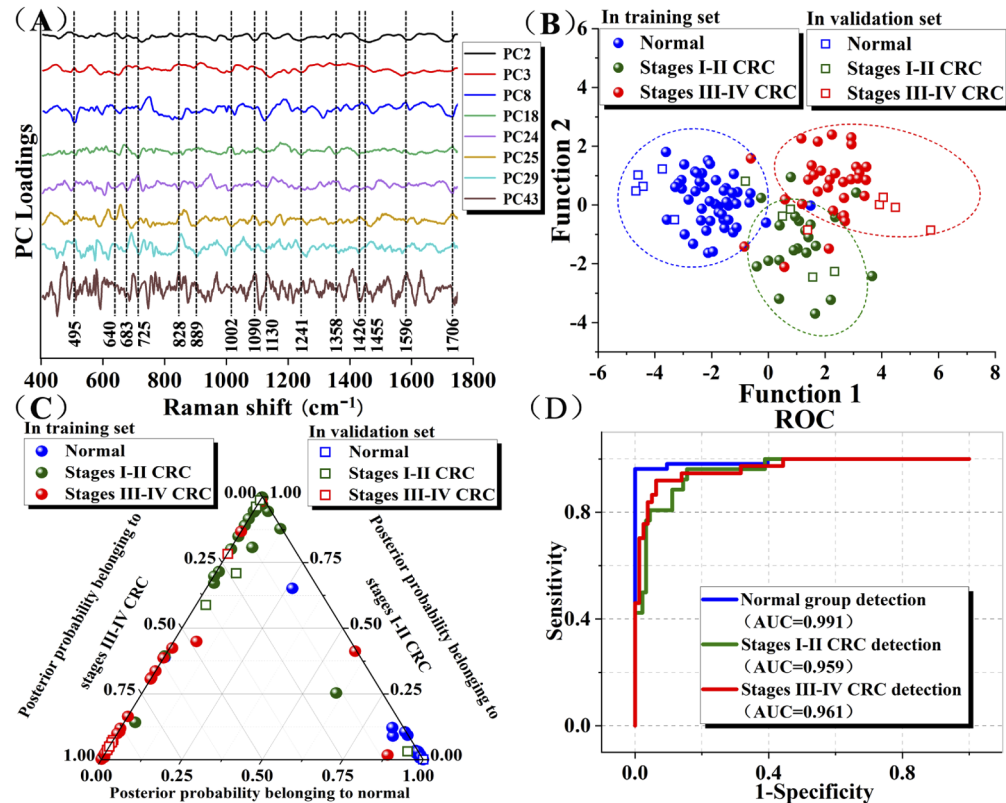


Fig. 4. (A) The most diagnostically significant PC loadings plot ($p < 0.05$). (B) Scatter plot of the discrimination scores and (C) two-dimensional ternary plot of the posterior probabilities for training dataset and validation dataset. (D) Receiver operating characteristic (ROC) curves of classification results for the three groups generated from PCA-DFA analysis. The integration areas under the ROC curves (AUC) are 0.991, 0.959 and 0.961, respectively, for the three groups' classification.

Table 3. Classification results of SERS spectra prediction of the three urine types in training dataset

Table Urine types	Predicted Groups		
	Normal group	Stages I and II CRC	Stages III and IV CRC
Normal	46	1	1
Stage I and II CRC	1	17	3
Stage III and IV CRC	2	3	27
Sensitivity (%)	95.8 (46/48)	80.9 (17/21)	84.3 (27/32)
Specificity (%)	94.3 (50/53)	95.0 (76/80)	94.2 (65/69)

4. Conclusion

In summary, a potential label-free urine test based on SERS was developed to analyze human urine for CRC detection at early and advanced stages. This study showed that there were significant spectral differences among normal, stages I-II CRC, and stages III-IV CRC. Meanwhile, tentative assignments of the SERS bands indicated dysregulated metabolism of CRC urinary biomolecules, including urea, specific amino acids, nucleic acid bases and so on. The PCA-DFA algorithms were employed to classify SERS spectra of the three different urine types with good diagnostic sensitivities, illustrating the great potential of urine SERS for convenient and noninvasive detection of colorectal cancer. Our next step will focus on the following two important parts: (1) collecting urine samples from the below three groups: one consisted of cancer patients with the use of drugs; one consisted of cancer patients with complications; and one consisted of patients suffering from other diseases to study the effects from these factors in-depth; (2) collecting more SERS data from more specimens including colorectal polyps and other types of cancers to further evaluate the utility of this method for cancer detection.

Funding

National Natural Science Foundation of China (61975031, 11974077, 61575043, 81741008); The Innovation Team Development Plan, Ministry of Education (IRT_15R10); The Special Funds of the Central Government Guiding Local Science and Technology Development (17L3009, 2020L3008); United Fujian Provincial Health and Education Project for Tackling the Key Research, China (2019-WJ-03); Startup Fund for scientific research, Fujian Medical University (2017XQ1209); Natural Science Foundation of Fujian Province (2020J011121); The program for Industry-University Cooperation Project of Fujian Province (2020Y4006).

Disclosures

The authors declare that there are no conflicts of interest related to this article.

See [Supplement 1](#) for supporting content.

References

1. B. Freddie, F. Jacques, S. Isabelle, L. S. Rebecca, A. T. Lindsey, and J. Ahmedin, "Global cancer statistics 2018: GLOBOCAN estimates of incidence and mortality worldwide for 36 cancers in 185 countries," *CA Cancer J. Clin.* **68**(6), 394–424 (2018).
2. D. M. Kimberly, N. Leticia, B. M. Angela, H. R. Julia, K. R. Yabroff, M. A. Catherine, J. Ahmedin, L. K. Joan, and L. S. Rebecca, "Cancer treatment and survivorship statistics," *CA Cancer J. Clin.* **69**, 363–385 (2019).
3. Y. Gao, J. Wang, Y. Zhou, S. Sheng, S. Y. Qian, and X. Huo, "Evaluation of serum CEA, CA19-9, CA72-4, CA125 and ferritin as diagnostic markers and factors of clinical parameters for colorectal cancer," *Sci. Rep.* **8**(1), 2732 (2018).

4. C. Zong, M. Xu, L. J. Xu, T. Wei, X. Ma, X. S. Zheng, R. Hu, and B. Ren, "Surface-enhanced Raman spectroscopy for bioanalysis: reliability and challenges," *Chem. Rev.* **118**(10), 4946–4980 (2018).
5. D. Lin, Q. Wu, S. Qiu, G. Chen, S. Feng, R. Chen, and H. Zeng, "Label-free liquid biopsy based on blood circulating DNA detection using SERS-based nanotechnology for nasopharyngeal cancer screening," *Nanomedicine* **22**, 102100 (2019).
6. D. Lin, T. Gong, Z. Hong, S. Qiu, J. Pan, C. Tseng, S. Feng, R. Chen, and V. Kong, "Metal carbonyls for the biointerference-free ratiometric surface-enhanced Raman spectroscopy-based assay for cell-free circulating DNA of Epstein-Barr virus in blood," *Anal. Chem.* **90**(12), 7139–7147 (2018).
7. E. Prado, N. Daugey, S. Plumet, L. Servant, and S. Lecomte, "Quantitative label-free RNA detection using surface-enhanced Raman spectroscopy," *Chem. Commun.* **47**, 7425–7427 (2011).
8. I. Bruzas, W. Lum, Z. Gorunmez, and L. Sagle, "Advances in surface-enhanced Raman spectroscopy (SERS) substrates for lipid and protein characterization: sensing and beyond," *Analyst* **143**(17), 3990–4008 (2018).
9. X. Han, B. Zhao, and Y. Ozaki, "Surface-enhanced Raman scattering for protein detection," *Anal. Bioanal. Chem.* **394**(7), 1719–1727 (2009).
10. S. Feng, J. Lin, Z. Huang, G. Chen, W. Chen, Y. Wang, R. Chen, and H. Zeng, "Esophageal cancer detection based on tissue surface-enhanced Raman spectroscopy and multivariate analysis," *Appl. Phys. Lett.* **102**(4), 043702 (2013).
11. M. Velicka, M. Pucetaite, V. Urboniene, J. Ceponkus, F. Jankevicius, and V. Sablinskas, "Detection of cancerous kidney tissue by means of SERS spectroscopy of extracellular fluid," *J. Raman Spectrosc.* **48**(12), 1744–1754 (2017).
12. S. Feng, Z. Li, G. Chen, D. Lin, S. Huang, Z. Huang, Y. Li, J. Lin, R. Chen, and H. Zeng, "Ultrasound-mediated method for rapid delivery of nano-particles into cells for intracellular surface-enhanced Raman spectroscopy and cancer cell screening," *Nanotechnology* **26**(6), 065101 (2015).
13. Y. Yun, L. Juqiang, L. Duo, F. Shangyuan, C. Weiwei, H. Zufang, H. Hao, and C. Rong, "Leukemia cells detection based on electroporation assisted surface-enhanced Raman scattering," *Biomed. Opt. Express* **8**(9), 4108 (2017).
14. S. Feng, W. Wang, I. T. Tai, G. Chen, R. Chen, and H. Zeng, "Label-free surface-enhanced Raman spectroscopy for detection of colorectal cancer and precursor lesions using blood plasma," *Biomed. Opt. Express* **6**(9), 3494–3502 (2015).
15. X. Li, T. Yang, S. Li, L. Jin, D. Wang, D. Guan, and J. Ding, "Noninvasive liver diseases detection based on serum surface enhanced Raman spectroscopy and statistical analysis," *Opt. Express* **23**(14), 18361–18372 (2015).
16. S. Li, L. Li, Q. Zeng, Y. Zhang, Z. Guo, Z. Liu, M. Jin, C. Su, L. Lin, J. Xu, and S. Liu, "Characterization and noninvasive diagnosis of bladder cancer with serum surface enhanced Raman spectroscopy and genetic algorithms," *Sci. Rep.* **5**(1), 9582 (2015).
17. S. Huang, L. Wang, W. Chen, S. Feng, J. Lin, Z. Huang, G. Chen, B. Li, and R. Chen, "Potential of non-invasive esophagus cancer detection based on urine surface-enhanced Raman spectroscopy," *Laser Phys. Lett.* **11**(11), 115604 (2014).
18. D. Greta, C. Silvia, M. Elena, S. Riccardo, C. Alfonso, B. Pietro, Z. Renzo, S. Agostino, S. Valter, and B. Alois, "Surface-enhanced Raman spectroscopy of urine for prostate cancer detection: a preliminary study," *Anal. Bioanal. Chem.* **407**(12), 3271–3275 (2015).
19. J. Connolly, K. Davies, A. Kazakeviciute, A. Wheatley, P. Dockery, I. Keogh, and M. Olivo, "Non-invasive and label-free detection of oral squamous cell carcinoma using saliva surface-enhanced Raman spectroscopy and multivariate analysis," *Nanomedicine* **12**(6), 1593–1601 (2016).
20. D. Lin, S. Feng, J. Pan, Y. Chen, J. Lin, G. Chen, S. Xie, H. Zeng, and R. Chen, "Colorectal cancer detection by gold nanoparticle based surface-enhanced Raman spectroscopy of blood serum and statistical analysis," *Opt. Express* **19**(14), 13565–13577 (2011).
21. Y. Chen, G. Chen, S. Feng, J. Pan, X. Zheng, Y. Su, Y. Chen, Z. Huang, X. Lin, F. Lan, R. Chen, and H. Zeng, "Label-free serum ribonucleic acid analysis for colorectal cancer detection by surface-enhanced Raman spectroscopy and multivariate analysis," *J. Biomed. Opt.* **17**(6), 067003 (2012).
22. J. Wang, D. Lin, J. Lin, Y. Yu, Z. Huang, Y. Chen, J. Lin, S. Feng, B. Li, N. Liu, and R. Chen, "Label-free detection of serum proteins using surface-enhanced Raman spectroscopy for colorectal cancer screening," *J. Biomed. Opt.* **19**(8), 087003 (2014).
23. B. Song, S. Jain, S. Lin, Q. Chen, T. Block, W. Song, D. Brenner, and Y. Su, "Detection of hypermethylated vimentin in urine of patients with colorectal cancer," *J. Mol. Diagn.* **14**(2), 112–119 (2012).
24. Y. Zheng, J. Yang, X. Zhao, B. Feng, H. Kong, Y. Chen, S. Lv, M. Zheng, and G. Xu, "Urinary nucleosides as biological markers for patients with colorectal cancer," *World J. Gastroenterol.* **11**(25), 3871–3876 (2005).
25. J. Poole, C. Vibat, L. Benesova, B. Belsanova, S. Hancock, T. Lu, M. Erlander, and M. Minarik, "Highly sensitive quantitative detection of circulating tumor DNA in urine and plasma from advanced colorectal cancer patients in aid of early diagnosis of clinically relevant KRAS mutations," *Biochem. Pharmacol.* **28**, 1791–1799 (2015).
26. V. Moisoiu, A. Socaciu, A. Stefancu, S. Iancu, I. Boros, C. Alecsa, C. Rachieriu, A. Chiorean, D. Eniu, N. Leopold, C. Socaciu, and D. Eniu, "Breast cancer diagnosis by surface-enhanced Raman scattering (SERS) of urine," *Appl. Sci.* **9**(4), 806 (2019).
27. K. Grabar, R. Freeman, M. Hommer, and M. Natan, "Preparation and characterization of Au colloid monolayers," *Anal. Chem.* **67**(4), 735–743 (1995).

28. M. Amin, F. Greene, S. Edge, C. Compton, J. Gershenwald, R. Brookland, L. Meyer, D. Gress, D. Byrd, and D. Winchester, "The Eighth Edition AJCC Cancer Staging Manual: Continuing to build a bridge from a population-based to a more "personalized" approach to cancer staging," *CA: Cancer J. Clin.* **67**(2), 93–99 (2017).
29. R. Liu, X. Yang, W. Tang, G. Yan, X. Yan, and M. Si, "Near-infrared surface-enhanced Raman spectroscopy (NIR-SERS) studies on oxyhemoglobin (OxyHb) of liver cancer based on PVA-Ag nanofilm," *J. Raman Spectrosc.* **44**(3), 362–369 (2013).
30. J. Zhao, H. Lui, D. I. McLean, and H. Zeng, "Automated autofluorescence background subtraction algorithm for biomedical Raman spectroscopy," *Appl. Spectrosc.* **61**(11), 1225–1232 (2007).
31. Z. Huang, A. McWilliams, H. Lui, D. I. McLean, S. Lam, and H. Zeng, "Near-infrared Raman spectroscopy for optical diagnosis of lung cancer," *Int. J. Cancer* **107**(6), 1047–1052 (2003).
32. M. a. Martin, "Surface-enhanced spectroscopy," *Rev. Mod. Phys.* **57**(3), 783–826 (1985).
33. Q. Wu, S. Qiu, Y. Yu, W. Chen, H. Lin, D. Lin, S. Feng, and R. Chen, "Assessment of the radiotherapy effect for nasopharyngeal cancer using plasma surface-enhanced Raman spectroscopy technology," *Biomed. Opt. Express* **9**(7), 3413–3423 (2018).
34. S. Feng, Z. Zheng, Y. Xu, J. Lin, G. Chen, C. Weng, D. Lin, S. Qiu, M. Cheng, Z. Huang, L. Wang, R. Chen, S. Xie, and H. Zeng, "A noninvasive cancer detection strategy based on gold nanoparticle surface-enhanced raman spectroscopy of urinary modified nucleosides isolated by affinity chromatography," *Biosens. Bioelectron.* **91**, 616–622 (2017).
35. S. Feng, J. Lin, M. Cheng, Y. Li, G. Chen, Z. Huang, Y. Yu, R. Chen, and H. Zeng, "Gold nanoparticle based surface-enhanced Raman scattering spectroscopy of cancerous and normal nasopharyngeal tissues under near-infrared laser excitation," *Appl. Spectrosc.* **63**(10), 1089–1094 (2009).
36. J. De Gelder, K. De Gussem, P. Vandenabeele, and L. Moens, "Reference database of Raman spectra of biological molecules," *J. Raman Spectrosc.* **38**(9), 1133–1147 (2007).
37. Z. Movasaghi, S. Rehman, and I. Rehman, "Raman Spectroscopy of Biological Tissues," *Appl. Spectrosc. Rev.* **42**(5), 493–541 (2007).
38. C. Westley, Y. Xu, B. Thilaganathan, A. J. Carnell, N. J. Turner, and R. Goodacre, "Absolute quantification of uric acid in human urine using surface enhanced Raman scattering with the standard addition method," *Anal. Chem.* **89**(4), 2472–2477 (2017).
39. A. Hussain, D. W. Sun, and H. Pu, "SERS detection of urea and ammonium sulfate adulterants in milk with coffee ring effect," *Food Additives & Contaminants: Part A* **36**(6), 851–862 (2019).
40. M. Li, Y. Du, F. Zhao, J. Zeng, C. Mohan, and W. Shih, "Reagent- and separation-free measurements of urine creatinine concentration using stamping surface enhanced Raman scattering (S-SERS)," *Biomed. Opt. Express* **6**(5), 849–858 (2015).
41. M. Tomizawa, F. Shinozaki, R. Hasegawa, Y. Shirai, Y. Motoyoshi, T. Sugiyama, S. Yamamoto, and N. Ishige, "Higher serum uric acid levels and advanced age are associated with an increased prevalence of colorectal polyps," *Biomed. Rep.* **3**(5), 637–640 (2015).
42. Y. Cheng, G. Xie, T. Chen, Y. Qiu, X. Zou, M. Zheng, B. Tan, B. Feng, T. Dong, P. He, L. Zhao, A. Zhao, L. Xu, Y. Zhang, and W. Jia, "Distinct urinary metabolic profile of human colorectal cancer," *J. Proteome. Res.* **11**(2), 1354–1363 (2012).
43. S. Barranco, R. Perry, M. Durm, M. Quraishi, A. Werner, S. Gregorcyk, and P. Kolm, "Relationship between colorectal cancer glutathione levels and patient survival: early results," *Dis. Colon Rectum* **43**(8), 1133–1140 (2000).
44. Y. Qiu, G. Cai, M. Su, T. Chen, Y. Liu, Y. Xu, Y. Ni, A. Zhao, S. Cai, L. Xu, and W. Jia, "Urinary metabonomic study on colorectal cancer," *J. Proteome Res.* **9**(3), 1627–1634 (2010).
45. W. Hsu, W. Chen, W. Lin, F. Tsai, Y. Tsai, C. Lin, W. Lo, L. Jeng, and C. Lai, "Analysis of urinary nucleosides as potential tumor markers in human colorectal cancer by high performance liquid chromatography/electrospray ionization tandem mass spectrometry," *Clin. Chim. Acta* **402**(1-2), 31–37 (2009).
46. H. L. Zhang, A. H. Zhang, J. H. Miao, H. Sun, G. L. Yan, F. F. Wu, and X. J. Wang, "Targeting regulation of tryptophan metabolism for colorectal cancer therapy: A systematic review," *RSC Adv.* **9**(6), 3072–3080 (2019).
47. W. Huang, D. Hopper, R. Goodacre, M. Beckmann, A. Singer, and J. Draper, "Rapid characterization of microbial biodegradation pathways by FT-IR spectroscopy," *J. Microbiol. Methods* **67**(2), 273–280 (2006).
48. R. Bro and A. K. Smilde, "Principal component analysis," *Anal. Methods* **6**(9), 2812–2831 (2014).
49. K. Varmuza and P. Filzmoser, "Introduction to multivariate statistical analysis in chemometrics," *Appl. Spectrosc.* **66**, 112 (2009).
50. K. Lin, D. Cheng, and Z. Huang, "Optical diagnosis of laryngeal cancer using high wavenumber Raman spectroscopy," *Biosens. Bioelectron.* **35**(1), 213–217 (2012).
51. N. Obuchowski, "Receiver operating characteristic curves and their use in radiology," *Radiology* **229**(1), 3–8 (2003).